Multilayer Silicon Nitride-on-Silicon Integrated Photonic Platform for 3D Photonic Circuits

Wesley D. Sacher[1], Zheng Yong[1], Jared C. Mikkelsen[1], Antoine Bois[1], Yisu Yang[1], Jason C. C. Mak[1], Patrick Dumais[2], Dominic Goodwill[2], Chaoxuan Ma[1], Junho Jeong[1], Eric Bernier[2], Joyce K. S. Poon[1]

[1]*Department of Electrical and Computer Engineering, University of Toronto, 10 King's College Road, Toronto, Ontario M5S 3G4, Canada*

[2]*Huawei Technologies Canada Co. Ltd., Suite 400, 303 Terry Fox Drive, Kanata, Ontario K2K 3J1, Canada*

wsacher@caltech.edu, joyce.poon@utoronto.ca

Abstract: A photonic platform with two passive silicon nitride layers atop an active silicon layer is demonstrated. It supports ultra-low loss (< 0.003dB) and crosstalk (< -52dB) crossings and efficient depletion modulation diodes with $V_\pi L$ of 2.6 V-mm.

OCIS codes: (130.0130) Integrated optics; (130.2790) Guided waves

1. Introduction

Silicon (Si) photonics enable large-scale photonic integrated circuits (PICs) due to the availability of large substrates and robust manufacturing flows. Applications requiring very-large-scale integration (VLSI) of 100s and 1000s of devices include optical switch fabrics [1], optical phased arrays [2], and coherent transceivers with several degrees of multiplexing [3-5]. Photonic VLSI necessitates complex on-chip waveguide networks to route the light between devices. Such interconnects must have low-loss waveguides and crossings with low loss and crosstalk. Here, we propose a three-dimensional (3D) platform for photonic VLSI, consisting of multiple interconnect waveguide layers and an active device layer. Critically, multiple layers enable low-loss and low-crosstalk crossings, wherein light in the topmost (bottommost) waveguide can cross over (under) a large number of waveguides. However, two-layer over/under-pass crossings [6-8] suffer from a trade-off between loss and crosstalk, since the waveguide layers must be close to each other for efficient interlayer transitions, yet far apart to reduce crossing loss and crosstalk. Crossing losses can readily dominate over interlayer and input/output coupling losses. Interlayer transition loss < 0.05 dB can be achieved [9], yet two-level crossings have 0.01-0.16 dB of loss [6-8].

To overcome this trade-off, we report a 3-layer active Si photonic platform on 8" SOI with two passive silicon nitride (SiN) waveguide layers on an active Si device layer for the O-band. The platform was fabricated at A*STAR Institute of Microelectronics. The lower SiN layer (SiN1) provides an intermediary transition between the Si layer and the upper SiN layer (SiN2), so a large interlayer spacing can be achieved with compact and low-loss interlayer transitions (Fig. 1(a)). The active Si layer contains efficient modulation diodes and photodetectors (PDs). This is the first demonstration of a foundry-fabricated 3-layer active Si photonic platform.

2. Multilayer Silicon Nitride-on-Silicon Integrated Photonic Platform

The cross-section of the multilayer platform is illustrated in Fig. 1(b). The platform has two 450 nm thick SiN layers separated by 200 nm thick SiO_2 spacers atop a 150 nm thick Si layer. The Si layer contains modulation diodes and Ge PDs. M1 and M2 are low resistivity metals, and TiN is for thin film heaters. Deep trenches formed thermal isolation regions around the heaters and edge couplers. Fig. 1(c) shows scanning electron micrographs of the tips of the adiabatic interlayer transitions in Si, SiN1, and SiN2. Non-uniform planarization over SiN1 led to the non-flat surface in Fig. 1(c) [bottom] and excess losses in the SiN2 layer. This issue has been resolved in an ongoing run. Nonetheless, the main features of this platform are demonstrated here. Fig. 1(d) shows the waveguide cutback structures and microring modulator reported below.

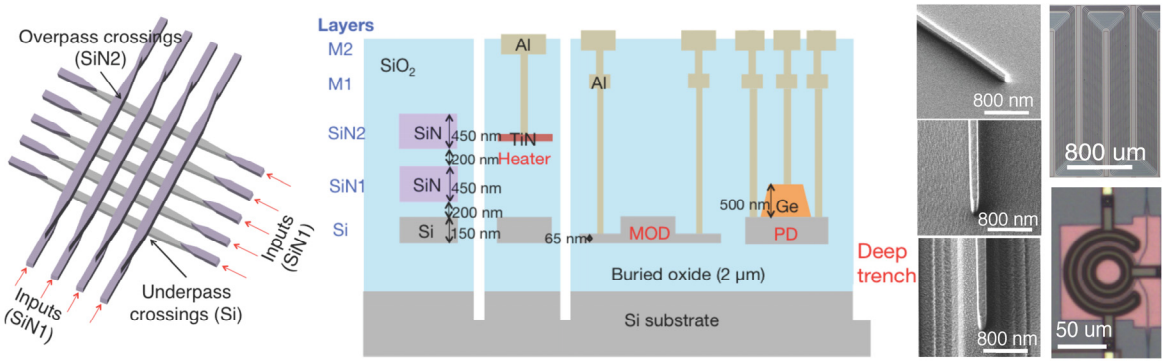

Fig. 1: (a) Illustration of the over/under-pass crossings in a multilayer photonic platform. (b) Schematic of the cross-section of the designed platform. Doping implantations are not shown. The platform has three waveguide layers (Si, SiN1, SiN2), two metal interconnect levels (M1, M2), TiN thin film heaters, depletion modulators (MOD), and Ge PD. (c) Tips of the interlayer transitions in the (top) Si, (centre) SiN1, and (bottom) SiN2 layers. (d) Optical micrographs of (top) cutback structures and (bottom) Si microring MOD.

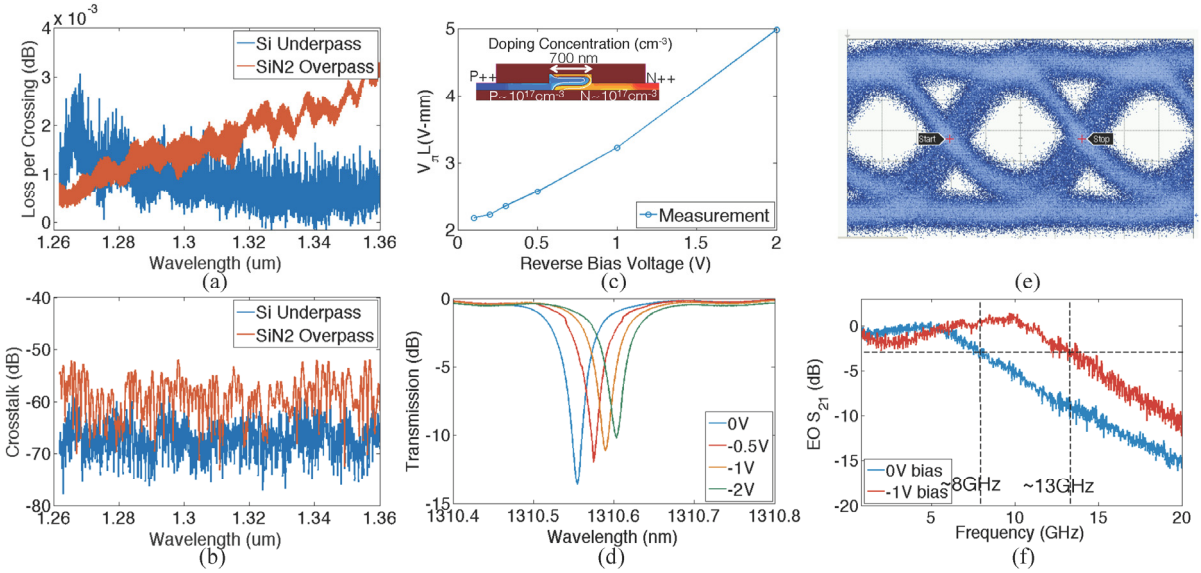

Fig. 2: Measured (a) loss and (b) crosstalk spectrum of the Si underpass and SiN2 overpass crossing at 90°. The loss and crosstalk are less than 3.4×10^{-3} dB and -52 dB, respectively. (c) The measured $V_\pi L$ vs. reverse bias from a MZI. Inset: TCAD simulated doping concentration of the designed modulation PN diode. The blue regions are P-type. (d) Microring transmission at several biases. (e) 13Gb/s eye pattern of a microring modulator with a drive voltage of $1.6V_{pp}$ at 0V bias. (f) The EO S21 of the microring modulator.

3. Device Characteristics

In terms of passive devices, the platform contains low-loss crossings and efficient heaters. Fig. 2(a) and (b) show the loss and crosstalk spectra of the SiN2 overpass and Si underpass crossings at 90° for the transverse electric (TE) polarization. The widths of the SiN2 and Si waveguides were 740 nm and 380 nm, respectively. Using cutback structures with up to 1600 crossings, over the O-band, the losses were < 3.4×10^{-3} dB for the overpass crossing and < 3.1×10^{-3} dB for the underpass crossing. The crosstalk was < -52 dB and < -58 dB for the overpass and underpass crossings, respectively. The underpass has less loss and crosstalk, because the optical mode is more confined in Si than SiN2. These results set a record for crossing loss and crosstalk in Si photonics. The π phase-shift tuning power of the thermal tuners was $P_\pi = 14$ mW, similar to high efficiency doped Si heaters that directly heat waveguides [10].

For the active devices, the platform contains efficient modulation diodes and photodetectors. PN junctions with the designed doping profile in the inset of Fig. 2(c) were implemented [11, 12]. The DC $V_\pi L$ extracted from a Mach-Zehnder modulator (MZM) test structure is shown in Fig. 2(c). At a reverse bias of 0.5V, the $V_\pi L$ was 2.6 V-mm, competitive with SISCAP MZMs (2V-mm in the O-band [13]), with the advantage that this diode can also be used in microrings. Fig. 2(d)-(f) show the results of a microring modulator with a diameter of 65 μm using this junction. The tuning efficiency of the microring was 40 pmV^{-1} between 0 and -0.5V. Fig. 2(e) shows an open eye pattern for the modulator at 13 Gb/s (PRBS 2^{31}-1) at a wavelength of 1310.58 nm. The extinction ratio was 10 dB and the device insertion loss was 2.5 dB. A drive voltage of only $1.6V_{pp}$ at 0V bias was applied to a terminated probe. The bit rate was partly limited by the microring linewidth of 50 pm (8.6 GHz). The electro-optic (EO) S_{21} in Fig. 2(f) taken near the -2.55 dB transmission point (to match the insertion loss) shows the 3dB bandwidth was ~8 GHz at 0V bias, extending to ~13 GHz at a bias of -1V. The Ge PD (not shown) has a length of 10 μm. At a -2V bias, the responsivity was 0.85 A/W at 1310 nm, the dark current was ~2 μA, and the 3dB bandwidth was ~16 GHz.

4. Conclusion

We have presented a multilayer Si photonics platform with two passive SiN layers on an active Si device layer containing low-loss crossings, efficient thermal tuners, optimized PN modulation junctions, and responsive photodetectors. This platform and extension to more layers open an avenue toward monolithic 3D photonic circuits.

Acknowledgments – We thank Drs. Y. Huang, X. Luo, and G.-Q. Lo of A*STAR Institute of Microelectronics for their technical assistance and the wafer fabrication.

5. References

[1] B. G. Lee *et al.*, *J. Lightwave Technol.*, 32(4), 743-751, 2014.
[2] J. Sun *et al., Nature*, 493, 195-199, 2013.
[3] P. Dong *et al.*, *J. Sel. Top. Quant. Electron.*, 20: 150-157, 2014.
[4] L. Chen *et al.*, *IEEE Photon. Technol. Lett.*, 23(13): 869-871, 2011.
[5] D. J. Richardson, *et al.*. *Nat. Photon.*, 7, 354-362, 2013.
[6] A. M. Jones *et al.*, *Opt. Express*, 21: 12002-12013, 2013.
[7] K. Shang *et al.*, *Opt. Express*, 23: 21334, 2015.
[8] T. J. Seok *et al.*, OFC, 2015. Paper M2B.4.
[9] W. D. Sacher *et al., J. Lightwave Technol.*, 33: 901-910, 2015.
[10] M. R. Watts *et al.*, *Opt. Lett.*, 38: 733-735, 2013.
[11] T. Cao *et al.*, *Appl. Optics*, 52(24): 5941-5948, 2013.
[12] Y. Liu *et al.*, *J. Lightwave Technol.*, 31(23): 3787-3793, 2013.
[13] M. A. Webster et al., OFC, 2015. Paper W4H.3